Hindawi
International Journal of RF and Microwave Computer-Aided Engineering
Volume 2023, Article ID 3838897, 11 pages
https://doi.org/10.1155/2023/3838897

Research Article

Open-Circuit Fault Detection in a Single Conductor Transmission Line Using TM_0 Mode Launcher

Swati V. Yadav and Ashish Chittora

Electrical and Electronics Engineering Department, BITS Pilani, K. K. Birla Goa Campus, Goa, India

Correspondence should be addressed to Ashish Chittora; ashish.chittora22@gmail.com

Received 31 October 2022; Revised 27 February 2023; Accepted 27 March 2023; Published 3 April 2023

Academic Editor: Ashish Bagwari

A novel surface wave (SW) launcher design for power line fault detection is presented in this paper. The launcher is capable of converting TE_{10} to TM_0 mode and exciting SW signal at 5.5 GHz frequency with high efficiency, on a single conductor line. The average attenuation of 2 dB/m and front to back ratio of 19 dB are observed and verified by simulation and experiments. Effect of bend, nearby obstacles, and extra wire connection on SW propagation is also investigated by experiments, and corresponding S-parameter results are presented. The optimization of launcher design with dielectric window and conical back plate is also demonstrated. The proposed launcher is compact and lightweight and can be easily installed without damaging the conductor line. Close structure makes it capable of withstanding outdoor environmental conditions. Using this launcher, microwave signal can be efficiently transmitted and received over existing conductor lines such as live power lines, pipes, and HVAC ducts, and it can be used in applications such as power line communication, fault detection, and permittivity measurement.

1. Introduction

Transmission of communication signal is possible with wireless and wired means such as coaxial cable, parallel wire line, microstrip line, and CPW line. Another unique method to transmit a high frequency signal by single conductor transmission line (SCTL) was proposed by Sommerfeld [1]. Later, it was experimentally established by Goubau [2]. Therefore, SCTL is also popularly known as Goubau-line or G-line. A high frequency signal can propagate on a SCTL without significant attenuation in the form of surface wave (SW). This technique could be useful, where line of sight communication is not possible and other transmission lines become very lossy. Theoretical and experimental work on surface wave propagation over SCTL is extensively reported by many researchers [3–7]. The signal on SCTL propagates in the form of surface wave or TM mode (transverse magnetic). The dominant mode on SCTL is TM_0 mode, and higher-order modes are attenuated within a short distance from the surface wave launcher or exciter [3]. If SCTL is an unshielded line, surface wave fields are spread and attenuated in transverse direction from the wire axis. The wave also gets attenuated in longitudinal direction due to finite resistivity of the wire as well as the dielectric loss and leakage in the surrounding medium. Dielectric coating can be used on SCTL to confine the fields closer to the wire, but it increases the attenuation in longitudinal direction [8, 9]. Therefore, the coated wire is used as SCTL only at low microwave frequencies to reduce the interference of nearby objects, wires, or circuits. At higher microwave frequencies (above S-band), uncoated wires can be used as SCTL.

Surface wave launcher plays an important role in the overall efficiency of the fault detection system. Due to reciprocity, the SW launcher and receiver are identical structures, and the terms will be used interchangeably in this paper. Many horn-shaped designs have been proposed for SW launcher [2, 4, 10–13], as it helps to concentrate the field on the line and has a symmetrical shape around the wire. The horn needs to be fed with a coaxial cable, and suitable arrangement is required to keep the cable isolated from SCTL and to save it from electrical damage. In some applications such as power line communication and fault detection, it is required that the SCTL remain completely unaffected and isolated from the SW launching system. The SW

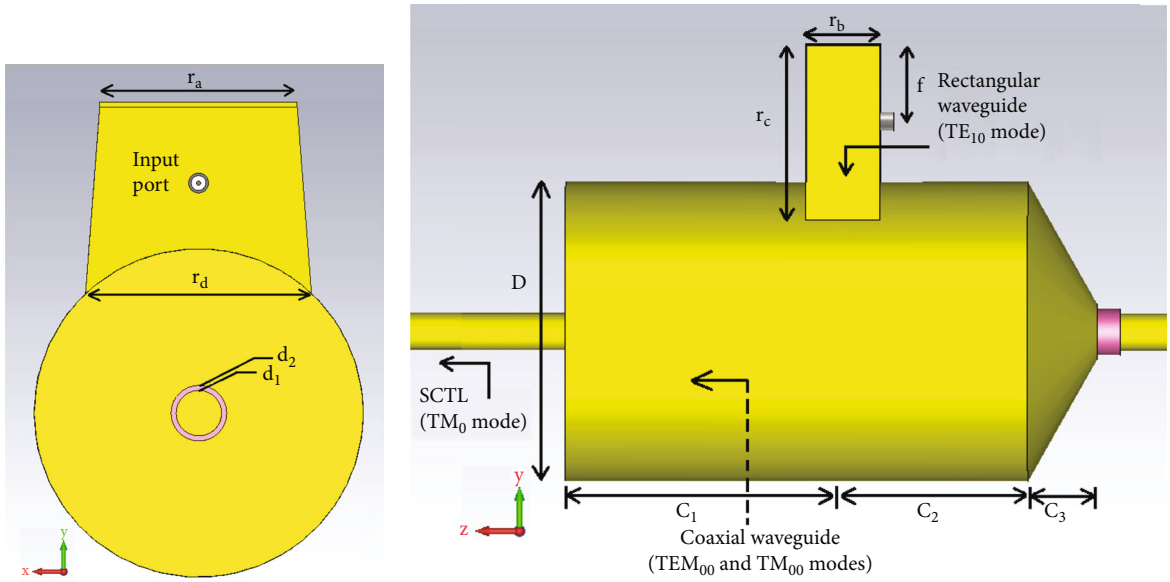

FIGURE 1: The design of the proposed surface wave launcher: (a) back view and (b) side view.

launcher should have provision to pass the SCTL wire through it and should be compact for maintaining mechanical stability and symmetry on wire.

SWTL has been used in many engineering applications and different launcher designs have been reported. In [10], a SWTL communication channel is proposed for long-range passive RFID application. The launcher is of horn shape, and a coupler is designed for feeding the communication signal to the launcher without affecting the original line. A horn-type SW exciter is reported in [11], with two port feeding structure. It is designed to adapt with the lines of different diameter. Utilization of classical antennas as surface wave launchers is investigated in [12, 13]. Experiments with double ridge horn antenna (DRHA) are demonstrated with single and double copper wire between them. 30-50 dB signal enhancement between antennas is observed relative to wireless link in short communication range (150 m). Although efficiency is high, the provision to pass the wire through antenna is not suggested.

In paper [14], a wire monopole and a wide monopole launcher are reported for power line fault detection. The ground plane is modified in folded form to improve the efficiency of the launcher. Planar designs of SW launcher are being reported to make it compatible with microstrip circuits [15–20]. A coplanar Vivaldi-type launcher is reported in [15], which can be installed on the existing power lines. This design is similar to a wire monopole fed with a CPW line. The CPW ground is extended in the form of Vivaldi structure on both sides of the monopole. A reflector is placed behind the launcher to mitigate the back propagated signal.

With the development of technology, many applications are utilizing the SW transmission line and launcher, such as fault detection [14], Terahertz communication [8, 16], biosensors [17, 18], leaky wave antennas [19, 20], dielectric constant measurement [21], and telemetry [22]. In the next section, the proposed surface wave launcher design and principle are discussed followed by the results and discussion in Section 3.

TABLE 1: Dimensions of the proposed SW launcher.

Parameter	Value	Parameter	Value
D	6.1 cm	C_1	6.0 cm
r_a	3.5 cm	C_2	4.0 cm
r_b	1.2 cm	C_3	1.5 cm
r_c	3.7 cm	d_1 (diameter)	0.8 cm
r_d	4.0 cm	d_2 (diameter)	1.0 cm
f (feed distance)	1.5 cm		

2. Launcher Design and Principle

The proposed surface wave launcher design is shown in Figure 1. The design consists of a circular waveguide, and on its side wall, a rectangular waveguide (RWG) is connected. The signal enters in the RWG through an SMA connector and an RF coaxial cable. Larger side of the RWG is slanted in the longitudinal direction for better coupling with the circular waveguide. One end of the circular waveguide is closed with a conical structure, which has an opening to pass the power cable (SCTL). Insulating material such as porcelain is used at the back end of circular waveguide between the power cable and conical structure.

Other end of the circular waveguide acts as the output port. Since the launcher structure requires mechanical support to stay firm on the power cable, a dielectric window or disc can be connected at the output port of the circular waveguide. Acrylic or Teflon is used as the dielectric window material with thickness 1 mm, and it also works as isolation between circular waveguide and power cable. However, other means can also be used to provide the mechanical

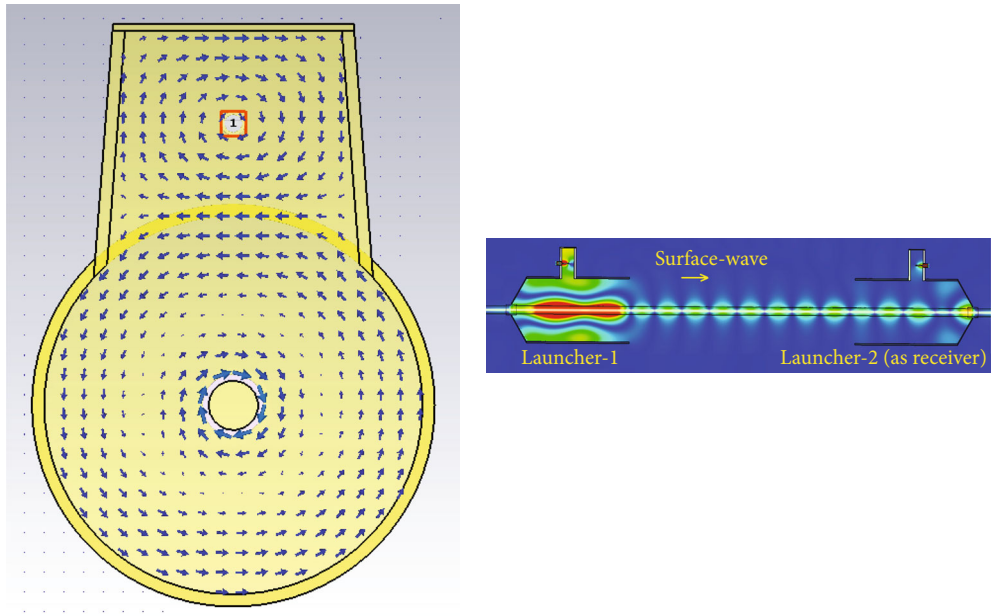

(a) (b)

FIGURE 2: Process of (a) rectangular TE_{10} to coaxial TEM mode coupling in the launcher and (b) surface wave propagation along the SCTL.

support, like dielectric thread or wire. When the power cable passes through the circular waveguide, it transforms into a coaxial structure. The dimensional details of the launcher design are given in Table 1.

The signal is excited in the rectangular waveguide with a metallic strip connected to the inner conductor of the SMA connector. The signal propagates as the dominant TE_{10} mode in the rectangular waveguide and consists of H-field loops surrounding the E-field lines. When H-field loops enter into the circular section, it couples with the coaxial waveguide structure as shown in Figure 2(a).

In a coax-WG, as the diameter ratio D/d_1 increases, the impedance of the TEM_{00} mode increases logarithmically and the real current density (J) in the center conductor tends toward zero [3]. Due to symmetry in coax-WG, only modes with a transverse magnetic field component (either TM or TEM) can propagate, since any asymmetric mode that produces a longitudinal magnetic field component will be attenuated immediately. Only the modes TEM_{0m} or TM_{0m} can propagate in a coax-WG. Additionally, for perfect conductors, energy may propagate only in the form of a hybrid of the principal modes and only TEM_{00} or TM_{00} modes are possible. Both of these principle modes propagate with same velocity, and it is determined by the relative permittivity (ε) of the dielectric material enclosed. If the coax-WG consists of perfect conductor and vacuum dielectric, both TEM_{00} and TM_{00} waves travel without attenuation at the speed of light. But the combined impedances and the combined admittances of the propagating modes are bounded such that for the total propagating wave,

$$Z_{\text{total}} = \frac{1}{Y_{\text{total}}} \leq \sqrt{\frac{\mu}{\varepsilon}},$$
$$Y_{\text{total}} = Y_{\text{TEM}_{00}} + Y_{\text{TM}_{00}} \geq \sqrt{\frac{\varepsilon}{\mu}} \approx 2.65 \times 10^{-3} \text{ mho}. \quad (1)$$

The admittance due to the TEM_{00} mode is continuous, positive, and finite in the range $1 < (D/d_1) < \infty$. So, for the case when $\ln(D/d_1) > 2\pi$, a propagating TM_{00} mode must also exist with a finite admittance:

$$\sqrt{\frac{\varepsilon}{\mu}} \leq Y_{\text{TM}_{00}} \leq \infty. \quad (2)$$

As a result, contrary to the conventional belief, in coax-cable or coax-WG, there exist simultaneously propagating TEM_{00} and TM_{00} modes over the entire range of coaxial geometries.

From the Maxwell-Heaviside equations, the total H-field in a coax-WG is due to both, the real current J_r involving moving free charges and the displacement current ($J_D = \varepsilon \partial E/\partial t$) due to the time rate of change of the E-field:

$$\nabla \times H = J_r + \varepsilon \frac{\partial E}{\partial t}. \quad (3)$$

At the transition from coax-WG to single conductor transmission line (SCTL), the outer conductor vanishes or can be assumed at infinity. The TM wave on an SCTL surrounded by a dielectric medium can be considered as a surface wave along the inner conductor of a coax-line having outer conductor at infinity (or very large diameter). In this view, for finite source voltage V_s, real current density (J_r) eliminates

$$J_r \longrightarrow 0 \text{ as } \frac{D}{d_1} \longrightarrow \infty. \quad (4)$$

When the outer conductor diameter of coax-WG increases without bound, the component of the H-field due to the longitudinal component of the displacement current

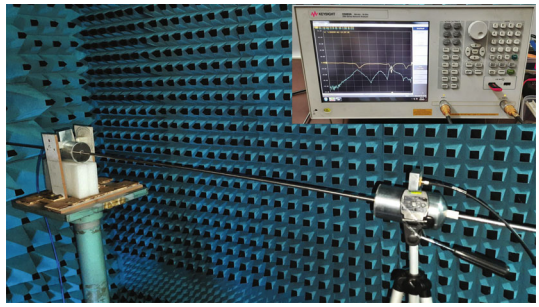

(a)

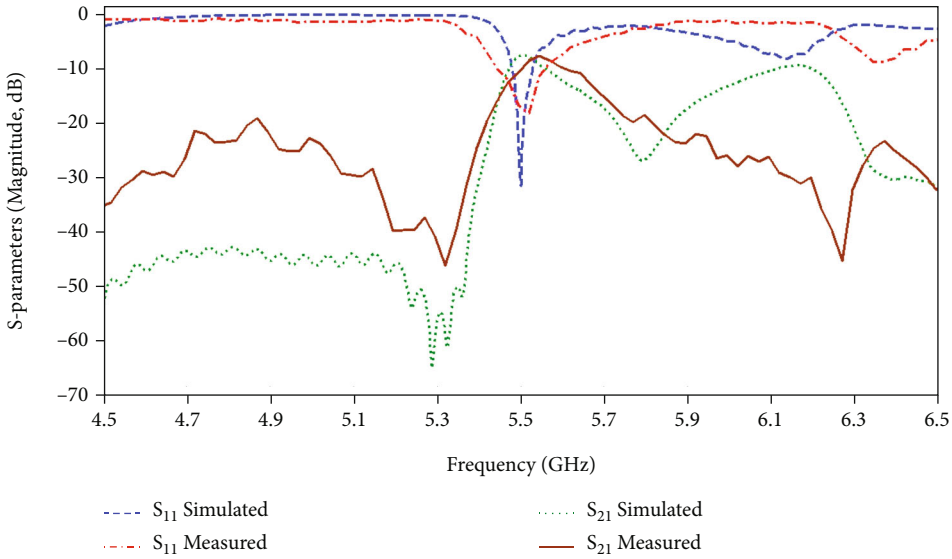

(b)

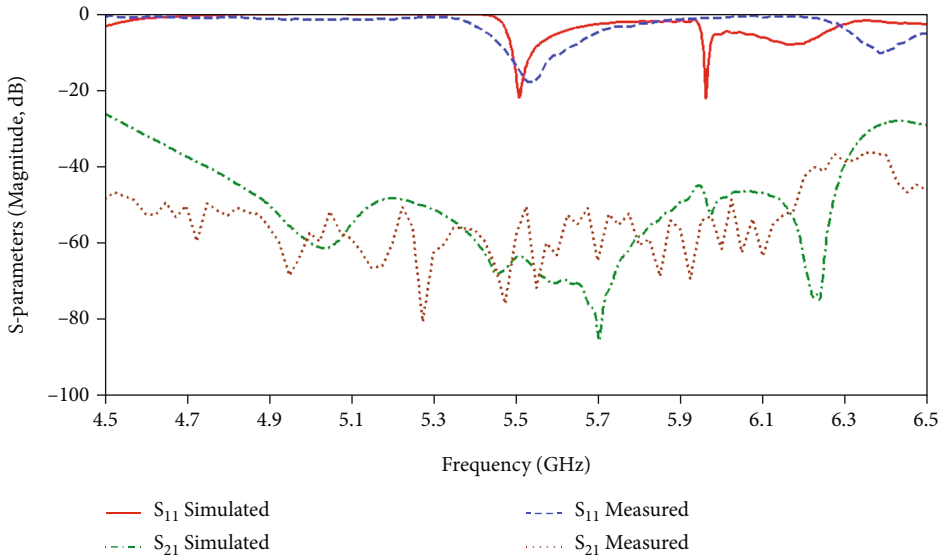

(c)

Figure 3: (a) Measurement setup and S-parameter results of the launcher (b) with SCTL and (c) without SCTL.

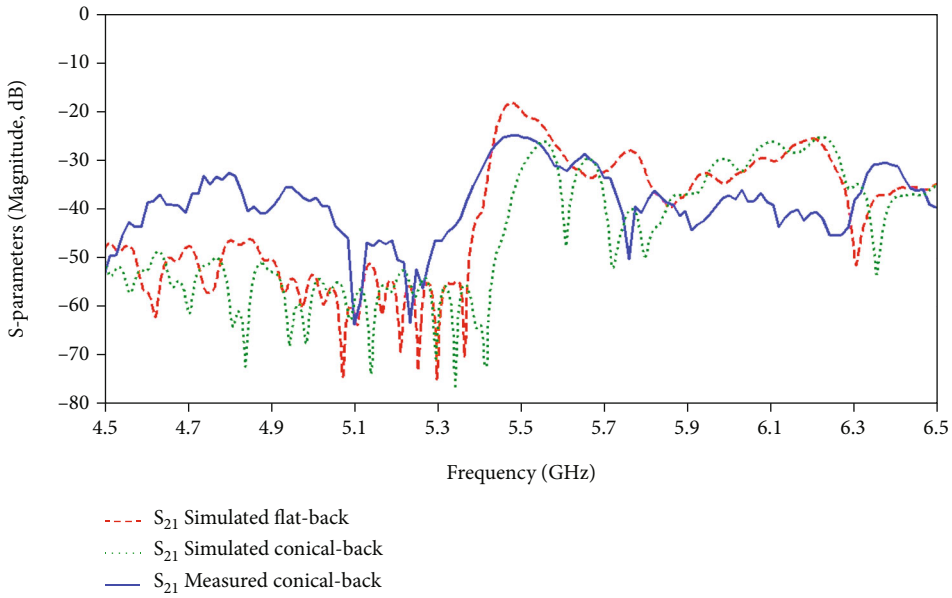

FIGURE 4: S-parameters of the launcher for signal propagated in backward direction of the launcher.

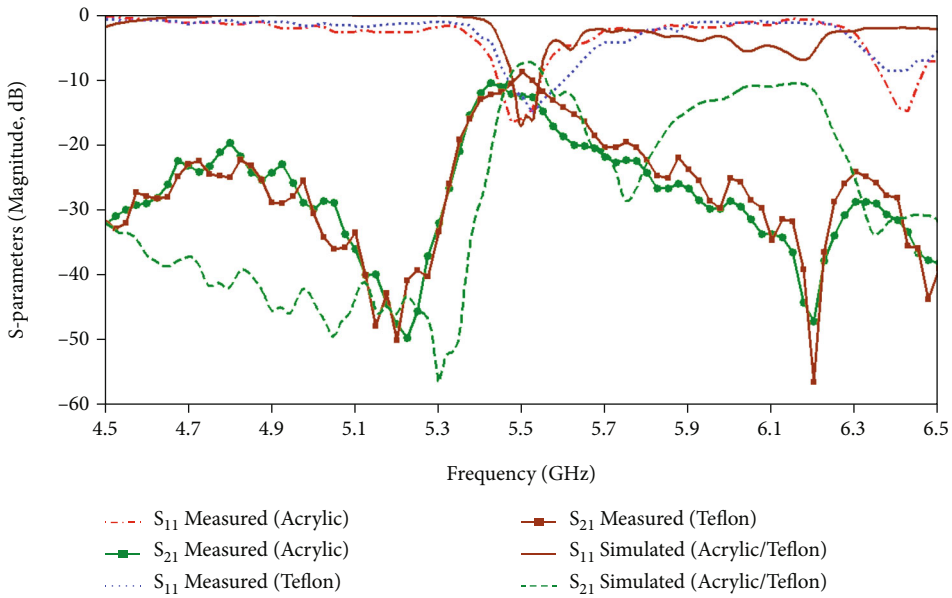

FIGURE 5: S-parameter results of the launcher with dielectric window (acrylic and Teflon) at the output port.

increases, and the component due to the real current decreases. As a result, TEM_{00} mode completely vanishes.

$$\frac{D}{d_1} \longrightarrow \infty,$$
$$Y_{\mathrm{TEM}} \longrightarrow 0, \tag{5}$$
$$Y_{\mathrm{total}} = Y_{\mathrm{TM}} = \sqrt{\frac{\varepsilon}{\mu}} \approx 2.65 \times 10^{-3}\ \mathrm{mho},$$

or

$$Z_{\mathrm{total}} = Z_{\mathrm{TM}} \approx 377\ \mathrm{ohm}. \tag{6}$$

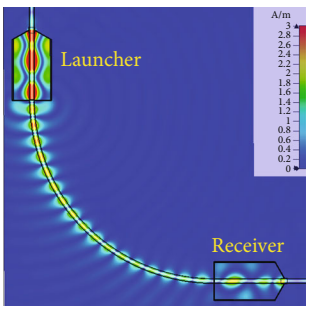

FIGURE 6: H-field propagation on a 90° bent SCTL.

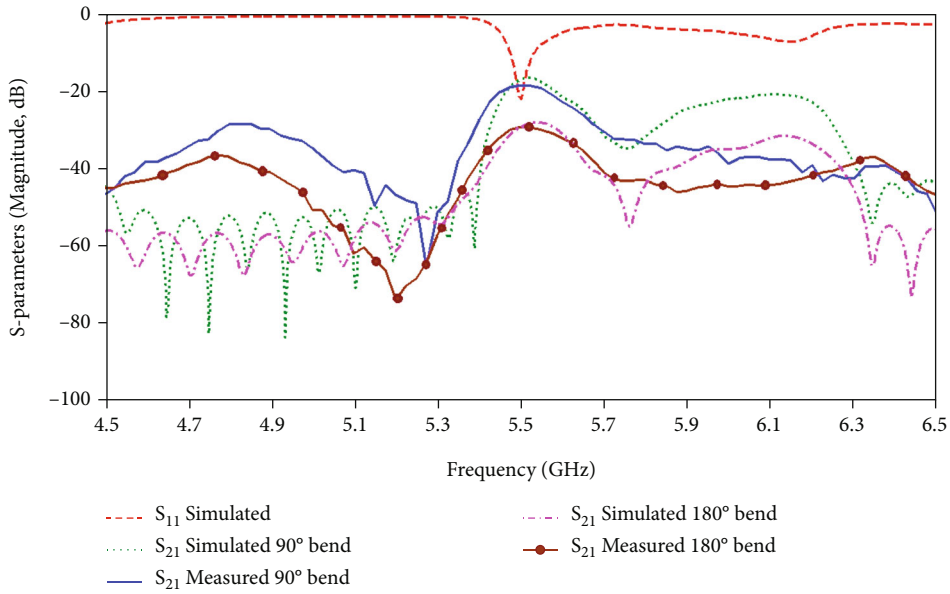

Figure 7: S-parameter results of the launcher for bent SCTL.

In the limit, the amount of real current in the outer conductor approaches to zero and the total admittance is completely due to the displacement current (J_D) which produces a single principal TM_{00} mode or TM_0 mode with the same free space wave impedance. This surface wave is received by Launcher-2 (or receiver), which has the same design as the Launcher-1 following the reciprocity theorem.

It is not required to make any change in the existing single conductor line to setup the SW launcher on it, and the SCTL is well isolated from the launcher parts. Unlike conventional SW launchers, this launcher design does not have horn part and is compact in size and shape with dimensions 6 cm × 9 cm × 11.5 cm. The simulated H-field propagation is shown, at a cross section of the launcher-receiver setup in Figure 2(b). Most of the surface wave fields are confined near the SCTL and are received by the receiver with minimum radiation losses.

3. Results and Discussion

3.1. S-Parameter Results of the Launcher. The surface wave launcher is designed and simulated in CST Microwave Studio software with 100 cm separation between the launchers. The material for launcher is taken as aluminium in simulation, as well as in fabrication with the dimensions shown in Figure 1 and Table 1. Aluminium cable with 8 mm diameter is taken as SCTL, and launchers are mounted on it, facing each other. Instead of solid cable, a metal pipe with smooth and conducting surface can also be used as SCTL. SMA female connectors at input ports of the launchers are connected to VNA through lossless coaxial cables for measurement. The rectangular waveguide section of the launcher is excited with a triangular shape (monopole) strip connected to inner conductor of SMA connector.

Measurement without SCTL is also performed to verify the existence of surface wave communication. Since the launcher radiates TEM mode at output port, there will be a minimum at the center of radiation pattern and no direct reception at line of sight direction. When the launchers are mounted on SCTL, the signal propagates as surface wave on the line and received with high efficiency by Launcher-2. It is also verified by connecting the launchers in cross-polarized orientation. S-parameter results are as shown in Figures 3(b) and 3(c) for comparison, with and without SCTL, respectively.

The S_{21}-parameter is more than 50 dB down at 5.5 GHz frequency in the absence of SCTL between launchers.

The effect of increasing the separation between launchers on the SCTL is investigated in the experiment. It is possible to estimate the average path loss of surface wave on the SCTL. The average path loss is calculated to be 2 dB/m.

3.2. Effect of Back Plate Shape on S-Parameters. Conventionally, flat metal plate is used to close the back of waveguides. In the initial launcher design with the flat back plate, the transmission efficiency was lower compared to the design with the conical back. The conical section at back of the launcher is an important element of the launcher design. This modification not only provides good in-phase superposition of the reflected fields in the front side but also reduces the back propagation of the signal. This improves the overall transmission efficiency of the surface wave propagation from the output port of the launcher.

Two launchers facing in the same direction are placed at a gap of 30 cm on the SCTL. Simulated and measured S_{21}-parameters for this setup are as shown in Figure 4. The peak of the simulated S_{21}-parameter for the flat back plate and the conical back is at -18 dB and -25 dB, respectively, at 5.5 GHz frequency, i.e., the improvement of 7 dB. Front to back ratio

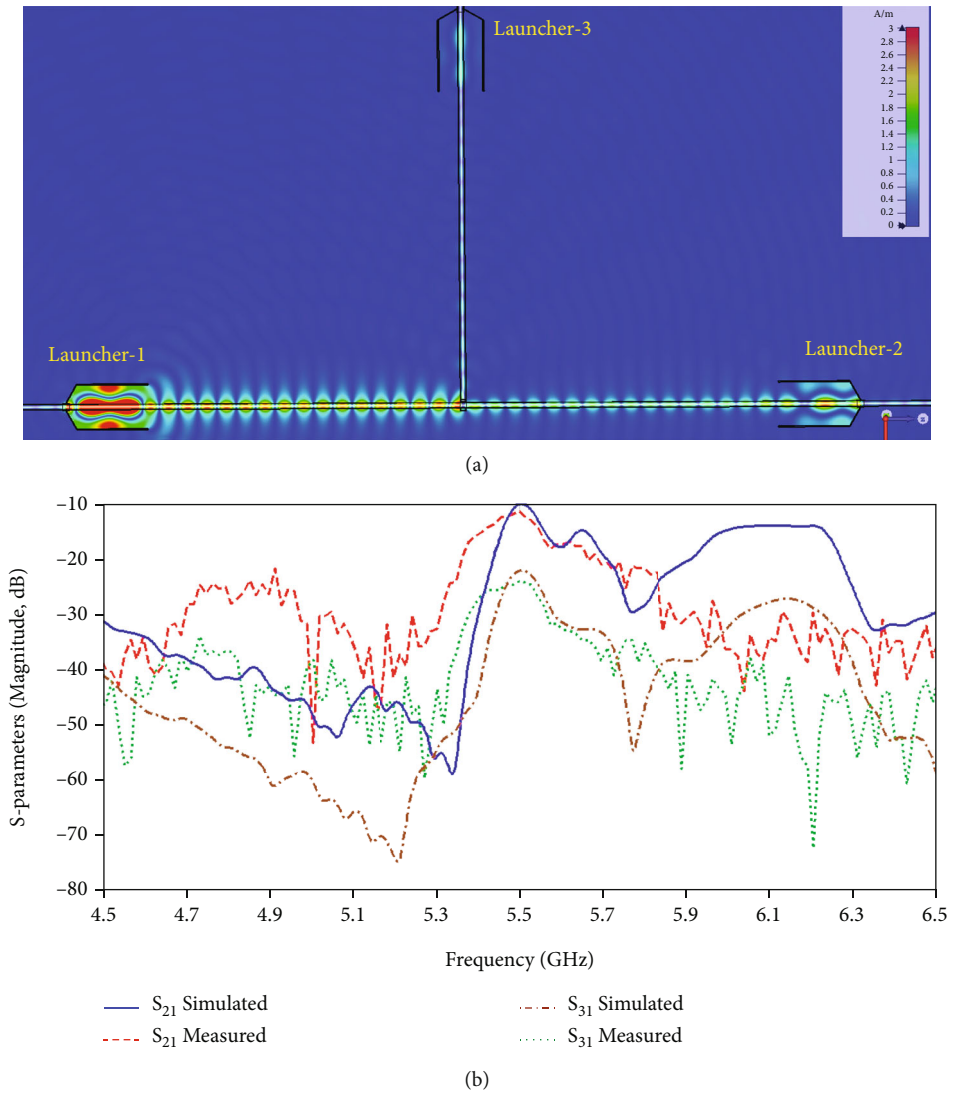

FIGURE 8: (a) H-field propagation in case of extra wire and Launcher-3 connected orthogonally on the SCTL between launchers and (b) corresponding S-parameter results.

is measured to be 19 dB for the launcher with conical back, for the launcher separation of 30 cm. This property is useful when one stage receiver and next stage launcher are connected back to back, to simultaneously operate two separate communication links. Measured back isolation will be higher, if the launchers are placed facing in opposite directions on the SCTL.

3.3. Effect of Dielectric Window on S-Parameters. In the proposed launcher design, output end of waveguide can be kept open and desired results are achieved. However, applying the dielectric window on the output port provides a mechanical support for the launcher on the SCTL and keeps the SCTL wire at the center of the launcher output port. It also protects the launcher from outdoor environmental conditions. Simulations are performed with acrylic and Teflon materials for dielectric window to calculate the optimized thickness. Windows of 1 mm acrylic and 2 mm Teflon are suitable. Experiments are performed with the dielectric window of both materials, and results are shown in Figure 5. It is observed that there is no degradation in S_{21}-parameter due to application of dielectric window.

3.4. Effect of Bending in SCTL on S-Parameters. In practical scenario, the overhead power lines or wires are not perfectly straight and may have sag or bend between the supporting poles. The sag in wire occurs due to thermal expansion, elasticity, and weight of the wire. Wire may be bent at some places due to mechanical deformation or change in the direction of poles. Simulation and measurement is performed to investigate the effect of sag and bend on the surface wave propagation. As an example, the sag of the curvature radius 100 cm is introduced in the wire (SCTL), and SW launchers are connected on both the ends. In practical situations, sag of such high curvature is very rare. No effect is observed on S-parameters in case of sagging in the wire.

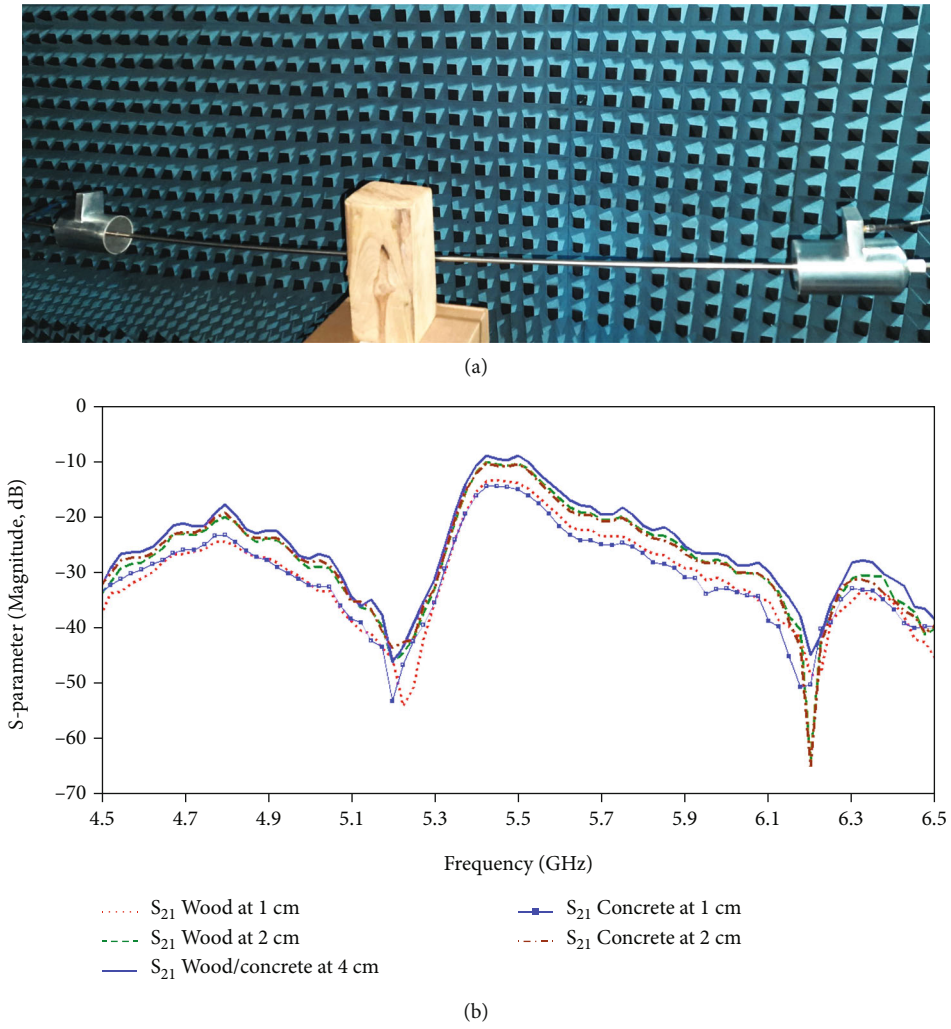

FIGURE 9: Measured S-parameter results of the launcher in the presence of wooden and concrete block near SCTL.

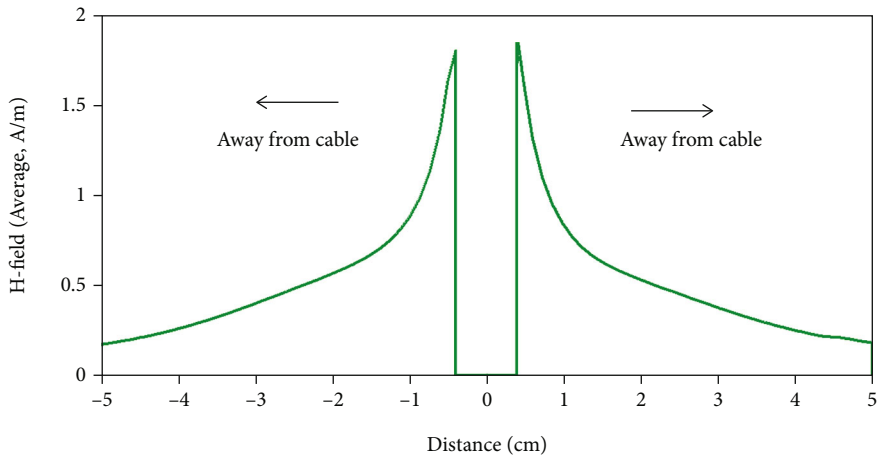

FIGURE 10: Simulated magnetic field decay in transverse direction away from the SCTL (cable) axis at 5.5 GHz frequency.

To investigate the effect of bending on S-parameters, two extreme bends of 90° and 180° angles are introduced in the wire. The radius of curvature is taken as 30 cm and axial length of SCTL is maintained as 100 cm between the launchers. From Figure 6, it is observed that the surface wave propagation exists on the line even in case of high curvature

bends. The corresponding S-parameter results are as shown in Figure 7. It is observed that there is a dip of 8 dB and 21 dB in S_{21}-parameter in case of 90° and 180° bends, respectively. The decrease in S_{21}-parameter peak is due to the radiation losses from the bend. The losses can be minimized by coating the wire with dielectric at the bend [8, 9]. The existence of surface wave on a bent SCTL makes it useful for nonline of sight communication.

3.5. Effect of Extra Wire on S-Parameters. Power lines also have the cross connection of other wires or lines. These extra wires can attenuate the SW signal propagating on the SCTL. This arrangement can also be used constructively to tap or extract the SW signal in orthogonal direction from the main SCTL. In this investigation, another SCTL is connected orthogonally at the center of main SCTL as shown in Figure 8(a). Launcher-3 is placed on the orthogonal line and S-parameters are measured. The simulation and measured results are shown in Figure 8(b), when the extra wire is connected at a distance of 50 cm from Launcher-1. It is also observed that the signal reception by Launcher-2 is better when discontinuity is away from Launcher-1. The level of signal received by Launcher-2 is decreased by 1.5 dB due to the extra wire, and a small SW signal reception on Launcher-3 is verified in simulated and measured S-parameter results.

3.6. Effect of Proximity of Objects on S-Parameters. The power distribution lines pass through different terrains which consist of trees, buildings, concrete poles, and other wires. Close proximity of these obstacles can attenuate the surface wave propagation on SCTL, if the SW fields are not closely bound to the wire. Experiments are performed to investigate the proximity effect of these obstacles on S-parameters of the launcher. Wooden and concrete blocks are placed near the wire as shown in Figure 9(a), and the distance from the wire is varied to investigate the effect. The distance up to which no effect is observed on S-parameters is 4 cm for both the cases.

If the object is brought closer than 4 cm, then the degradation in S_{21}-parameter is more in case of concrete relative to the wooden block as shown in Figure 9(b). This experiment also gives us an idea about the field spread or radial expansion around the SCTL. In this case, most of the SW fields are concentrated within 4 cm radius around the SCTL as shown in the simulated H-field plot in Figure 10. Dielectric coated line can be used to make the fields more concentrated near the wire [8, 9]. Field spread also decreases with the increasing frequency [13].

3.7. Fault Detection Measurement. The proposed SW launcher has a potential application of nonintrusive fault detection in unshielded power lines. Open-circuit faults can be detected using the time-domain reflectometry (TDR) technique. A Gaussian pulse of 2 ns width is generated on VNA and applied to the SW launcher input port. The launcher excites the TM_0 mode signal over the SCTL at one end, and other end of SCTL is kept open circuited. The signal is reflected from the open end, and it is detected by VNA in the time-domain measurement. Reflected signal is maximum when the transmission line is open or short circuited at the load end. Therefore, the peak of reflected signal can be used to calculate the distance of the open-circuit (fault) end.

Table 2: Open-circuit fault location measurement using SW launcher.

Return signal peak location t_1 (ns)	Measured length (m)	Actual length (m)	Error (%)
10.53	1.32	1.23	7.3
12.13	1.54	1.43	7.9
13.60	1.75	1.63	7.4
15.03	1.96	1.83	7.1
16.60	2.18	2.03	7.4
17.50	2.30	2.23	3.1
19.53	2.60	2.43	7.0
20.43	2.72	2.63	3.4
21.55	2.89	2.83	2.1
44.10	6.05	6.10	0.82
86.98	12.11	12.20	0.74
107.96	15.48	15.50	0.13
131.82	18.55	18.60	0.26

In this experiment, the distance of SW launcher from the open end is increased from 1.03 m to 2.83 m by 20 cm in each step. The reflected pulse is only observable after 1.23 m distance from the open end, else it is overlapped in the strong reflections of the launcher discontinuities. A comparison of the measured and actual distance of the open end from the launcher is presented in Table 2. The table includes the measurement data for the SW launcher distance from open end 1.23 m to 18.60 m. Average error of the each 20 cm shift of the launcher on SCTL is calculated from the measured results, and it comes out to be 5.85% for length below 6 m. The return signal plotted with respect to time is shown in Figure 11 for each 40 cm shift of SW launcher from the open-circuit fault end. The peak (near 0 ns) at $t_0 = 1.3$ ns is due to the internal reflections of the launcher and are not of interest. The second significant peak (t_1) is due to the signal reflected from the open end of the cable. The location of the fault can be calculated from the following formula:

$$L = \frac{kc(t_1 - t_0)}{2}, \tag{7}$$

where c is the speed of light (3×10^8 m/s) and k is the velocity factor. The value of k is between 0.7 and 0.8 for the shielded cables. For unshielded cables, the velocity factor can be taken as 0.95-0.98 [23]. In this work, the value of k is taken as 0.95 to take care of the losses due to finite conductivity, surface roughness, and other imperfections in SCTL. It is observed that the measurement error decreases for longer cables, but the amplitude of the return signal also

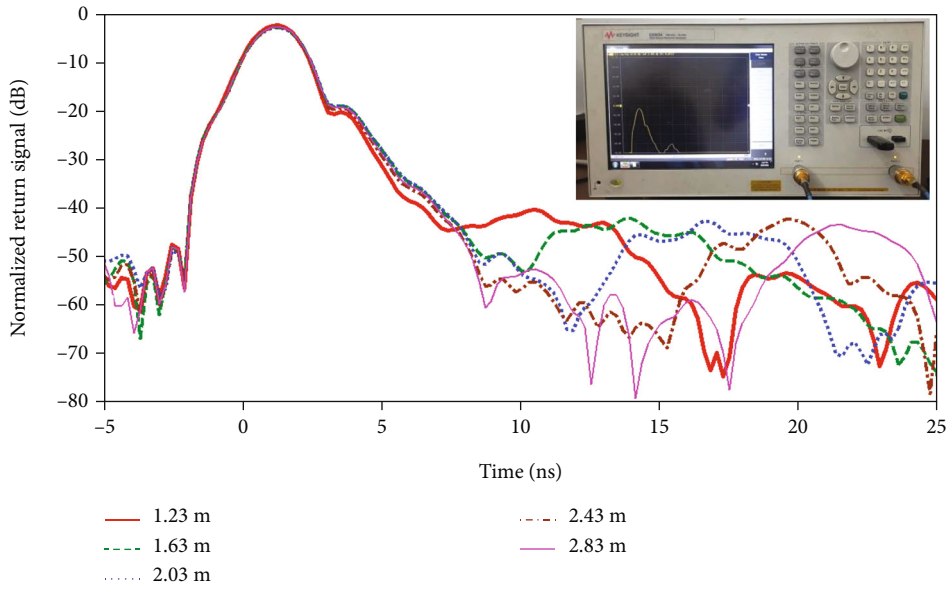

FIGURE 11: Reflected signal amplitude (normalized) of the SCTL open-circuit (at different distances) end in time-domain measurement at 5.5 GHz frequency.

decreases. The maximum error = 7.9% and average error = 4.2% are observed in the measurements.

4. Conclusion

A surface wave launcher design for rectangular TE_{10} to coaxial TEM to SW TM_0 mode is presented in this paper. The launcher is capable of exciting and receiving the surface wave signal on a single conductor transmission line efficiently at 5.5 GHz frequency. The simulated results are verified with experimentally measured results of the fabricated launcher in an anechoic chamber. The average path loss 2 dB/m is observed on 8 mm diameter SCTL (aluminium). The effect of sag and bend (90°) in the SCTL and the presence of nearby obstacles (at distance >4 cm) is minimum on the surface wave propagation. The SW signal level on the back side of the launcher is very low (-30 dB). Compact design and close structure make it convenient to install the launcher on the existing infrastructure such as power lines, pipes, cables, and ducts for transmitting the communication signal over power lines and other similar applications. The application of the SW launcher for open-circuit fault detection in unshielded power line is demonstrated with time-domain reflectometry experiment.

Conflicts of Interest

The authors declare that they have no conflicts of interest.

Acknowledgments

The authors are thankful to Prof. K. R. Anupama for providing the antenna measurement facility.

References

[1] A. Sommerfeld, *Electrodynamics*, Academic Press Inc, New York, 1952.

[2] G. Goubau, "Single-conductor surface-wave transmission lines," *Proceedings of the IRE*, vol. 39, no. 6, pp. 619–624, 1951.

[3] G. Elmore, "Introduction to the propagating wave on a single conductor," 2009, http://www.corridor.biz/FullArticle.pdf.

[4] G. Elmore, "A surface wave transmission line," 2012, http://www.sonic.net/~n6gn/ELMORE.pdf.

[5] H. Severin and G. Schulten, "Surface-wave transmission lines for microwave frequencies," *Phillips Technical Review*, vol. 26, pp. 342–350, 1965.

[6] P. S. Bhatnagar, "Surface wave transmission lines," *IETE Journal of Education*, vol. 17, no. 1, pp. 24–31, 1976.

[7] T. Schaich, D. Molnar, A. Al Rawi, and M. Payne, "Surface wave transmission line theory for single and many wire systems," *Journal of Applied Physics*, vol. 130, no. 19, article 194902, 2021.

[8] J. C. Wiltse, "Low-loss surface-wave propagation on coated or uncoated cylindrical conductor from 0.1 to 1 THz," in *2007 IEEE Antennas and Propagation Society International Symposium*, pp. 4657–4660, Honolulu, HI, USA, 2007.

[9] M. Wang, G. Wei, and R. Li, "Surface-wave transmission analysis on dielectric coated conducting wires," in *2018 International Applied Computational Electromagnetics Society Symposium-China (ACES)*, pp. 1-2, Beijing, China, 2018.

[10] A. Sharma, A. T. Hoang, and M. S. Reynolds, "Long-range battery-free UHF RFID with a single wire transmission line," *IEEE Sensors Journal*, vol. 17, no. 17, pp. 5687–5693, 2017.

[11] J. Liu, X. Li, B. Sun, J. Lan, and F. Zhao, "A surface wave exciter adapting to different-diameter lines and its application to single power line communications," *International Journal of RF and Microwave Computer-Aided Engineering*, vol. 30, no. 3, article e22102, 2020.

[12] T. Schaich, E. Dinc, D. Molnar et al., "Advanced modeling of surface waves on twisted pair cables: surface wave stopbands,"

IEEE Transactions on Microwave Theory and Techniques, vol. 70, no. 5, pp. 2541–2552, 2022.

[13] E. Dinc, A. A. Rawi, and E. de Lera Acedo, "Launching surface waves with classical antennas," in *ICC 2021- IEEE International Conference on Communications*, pp. 1–6, Montreal, QC, Canada, 2021.

[14] M. N. Alam, R. H. Bhuiyan, R. A. Dougal, and M. Ali, "Design and application of surface wave sensors for nonintrusive power line fault detection," *IEEE Sensors Journal*, vol. 13, no. 1, pp. 339–347, 2013.

[15] A. Sharma, A. T. Hoang, and M. S. Reynolds, "A coplanar Vivaldi-style launcher for Goubau single-wire transmission lines," *IEEE Antennas and Wireless Propagation Letters*, vol. 16, pp. 2955–2958, 2017.

[16] T. Akalin, A. Treizebre, and B. Bocquet, "Single-wire transmission lines at terahertz frequencies," *IEEE Transactions on Microwave Theory and Techniques*, vol. 54, no. 6, pp. 2762–2767, 2006.

[17] A. Treizebre, T. Akalin, and B. Bocquet, "Planar excitation of Goubau transmission lines for THz BioMEMS," *IEEE Microwave and Wireless Components Letters*, vol. 15, no. 12, pp. 886–888, 2005.

[18] J. S. Besnoff and S. Matthew, "Single-wire radio frequency transmission lines in biological tissue," *Applied Physics Letters*, vol. 106, no. 18, article 183705, 2015.

[19] K. Rudramuni, P. K. T. Rajanna, K. Kandaswamy, B. Majumder, and Q. Zhang, "Goubau line based end-fire antenna," *International Journal of RF and Microwave Computer-Aided Engineering*, vol. 29, no. 12, article e22008, 2019.

[20] Q. Zhang, X.-L. Tang, S. Hu, and Y. Chen, "A reconfigurable Goubau-line-based leaky wave antenna," in *2018 2nd URSI Atlantic Radio Science Meeting (AT-RASC)*, pp. 1–3, Gran Canaria, Spain, 2018.

[21] M. N. Alam, D. Coats, Y. Shin, R. A. Dougal, and M. Ali, "A new method to estimate the average dielectric constants of aged power cables," *Journal of Electromagnetic Waves and Applications*, vol. 28, no. 7, pp. 777–789, 2014.

[22] S. M. Amjadi and K. Sarabandi, "A compact single conductor transmission line launcher for telemetry in borehole drilling," *IEEE Transactions on Geoscience and Remote Sensing*, vol. 55, no. 5, pp. 2674–2681, 2017.

[23] A. O. Salman, "Phase velocity measurement of surface wave propagating along a Goubau-line: wire resonator method," in *IEEE EUROCON 2009*, pp. 57–63, St. Petersburg, Russia, 2009.